Preparation of Fluorinated Polyimides with Low Dielectric Constants, Low Dielectric Losses by Combining Ester Groups and Triphenyl pyridine Structures

Hong Li[a], Feng Bao*[a], Shuanger Li[a], Xiyan Li[a], Yadong Li[b], Kexin Mu[a], Mingliang Wang [a], Caizhen Zhu[a], Jian Xu*[a]

[a] Institute of Low-Dimensional Materials Genome Initiative, College of Chemistry and Environmental Engineering, Shenzhen University, Shenzhen, 518060, China.

[b] Chengdu Institute of Organic Chemistry, Chinese Academy of Sciences, Chengdu, 610041, P.R. China.

* Corresponding Authors

This supporting information is composed of a total of x pages, including y Figures.

1.1. Materials

1,3-Dioxo-1,3-dihydroisobenzofuran-5-carbonyl chloride (>98%) was purchased from Shanghai Bide Pharmaceutical Technology Co., Ltd. Acetic acid (AR) and acetic anhydride (AR) were purchased from Shenzhen Changtai Chemical Technology Co., Ltd. Bisphenol A (>98%), N, N-dimethylacetamide (DMAC, AR), acetonitrile (99.9%, H_2O <0.003%), pyridine were purchased from Shanghai Maclean Biochemical Technology Co., Ltd, where DMAC was treated by a solvent treatment system and used. Distilled water was homemade in the laboratory. All other unspecified drugs were purchased and used directly.

1.2. Measurements

The samples underwent rigorous NMR analysis involving nuclear magnetic resonance hydrogen spectroscopy (^{1}H NMR) and nuclear magnetic resonance carbon spectroscopy (^{13}C NMR). This assessment utilized an AVABCE III 500 MHz superconducting NMR spectrometer from Bruker in Switzerland. Internal standardization was achieved using tetramethylsilane (TMS), while DMSO-d6 was the chosen solvent. The temperature for testing was maintained at 25 °C. A Q Exactive

Focus mass spectrometer was deployed for the mass spectrometry examination. The samples' Fourier Transform Infrared Spectroscopy (FTIR) evaluation was conducted using the Shimadzu IR Affinity-1 instrument, covering a spectral range from 4000 cm^{-1} to 400 cm^{-1}. The molecular weight information of the polymers was characterized by a 1260 Infinity II GPC from Agilent Technologies. This analysis employed DMF and 0.1% LiCl as the mobile phases, with a 1.0 mL/min flow rate and a testing temperature of 45°C. A MiniFlex600 X-ray polycrystalline powder diffractometer from Japan was used for the WAXD analysis, focusing on a test angle range of 5° to 80°. The UV-visible assessment was performed using the UV-3600PLUS UV-visible near-infrared spectrometer by Shimadzu in Japan. Dielectric testing utilized the P5004A vector network analyzer from YesterTech, with a pre-testing drying treatment at 100 °C for 12 hours. The films were characterized by a thickness of 50 to 70 μm, and the test temperature was maintained at 25 °C. The contact angle test was carried out by the SDC-350 contact angle meter of Shengding Precision Instrument Company of Dongguan, and the sample was dried and processed at 100 ℃ for 5 h before the test. The thermals tests were conducted using METTLER TOLEDO's Mettler Differential Scanning Calorimeter (DSC3). The temperature range was 30-350 ℃, and the temperature increase was 20 ℃/min; the nitrogen gas flow rate was 50 ml/min. Determining thermal decomposition characteristics employed the Mettler Toledo Mettler TGA2 Thermogravimetric Analyzer. The tests encompassed a temperature range of 30 °C to 800 °C, with a temperature increase rate of 10 °C/min. Nitrogen and airflow were maintained at speeds of 50 ml/min. Mechanical properties were assessed using a Zwick tension machine with a 1 mm/min tension rate. The samples measured 20 mm × 6 mm, and the film thickness ranged from 50 to 70 μm. For the water absorption test, three sample films sized 50 mm × 50 mm underwent a vacuum oven drying at 120°C for 12 hours to establish mass W_1. Then the samples were submerged in distilled water for 24 hours, excess liquid was removed with a paper towel, and mass W_2 was measured. The resulting water absorption rate was calculated as $(W_2 - W_1) / W_1 \times 100$, and an average value was derived from three test repetitions.

Page S2:

Figure S1. (a) ^{1}H NMR spectra of BTPDA in DMSO-d_6, (b) ^{13}C NMR spectra of BTPDA in DMSO-d_6, (c) FTIR spectra of BTPDA

Figure S2. MS spectrum of BTPDA in DMF

Figure S3. ^{1}H NMR spectra of PAAs in DMSO-d_6

Figure S4. Dielectric properties of PI films under humid conditions

Figure S5. (a) GPC Date of PI-EH-PAA; (b) GPC Date of PI-ECF_3-PAA;(c) GPC Date of PI-E2CF_3-PAA

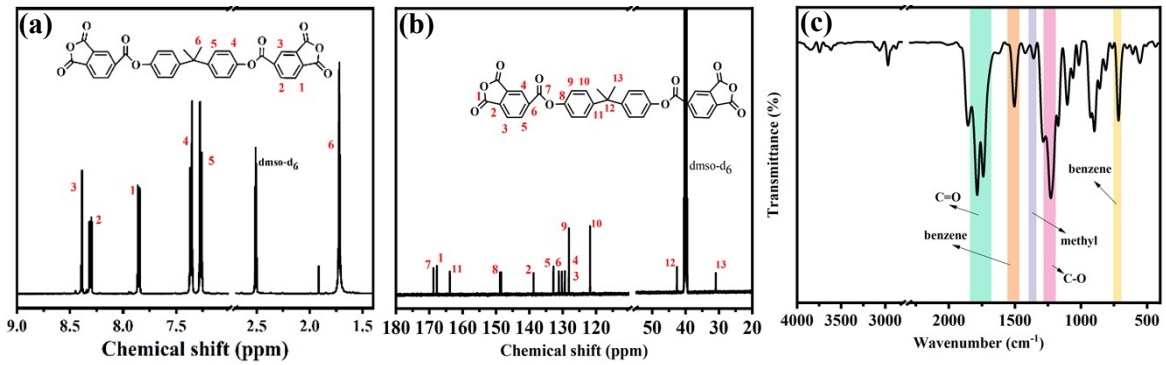

Figure S1. (a) ^{1}H NMR spectra of BTPDA in DMSO-d_6, (b) ^{13}C NMR spectra of BTPDA in DMSO-d_6, (c) FTIR spectra of BTPDA

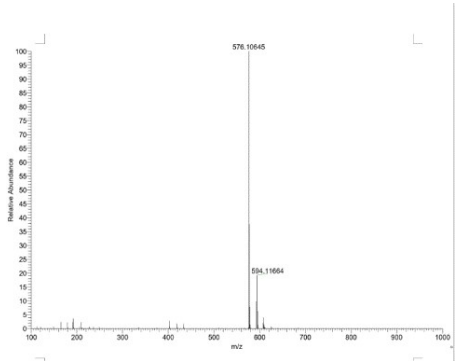

Figure S2. MS spectrum of BTPDA in DMF

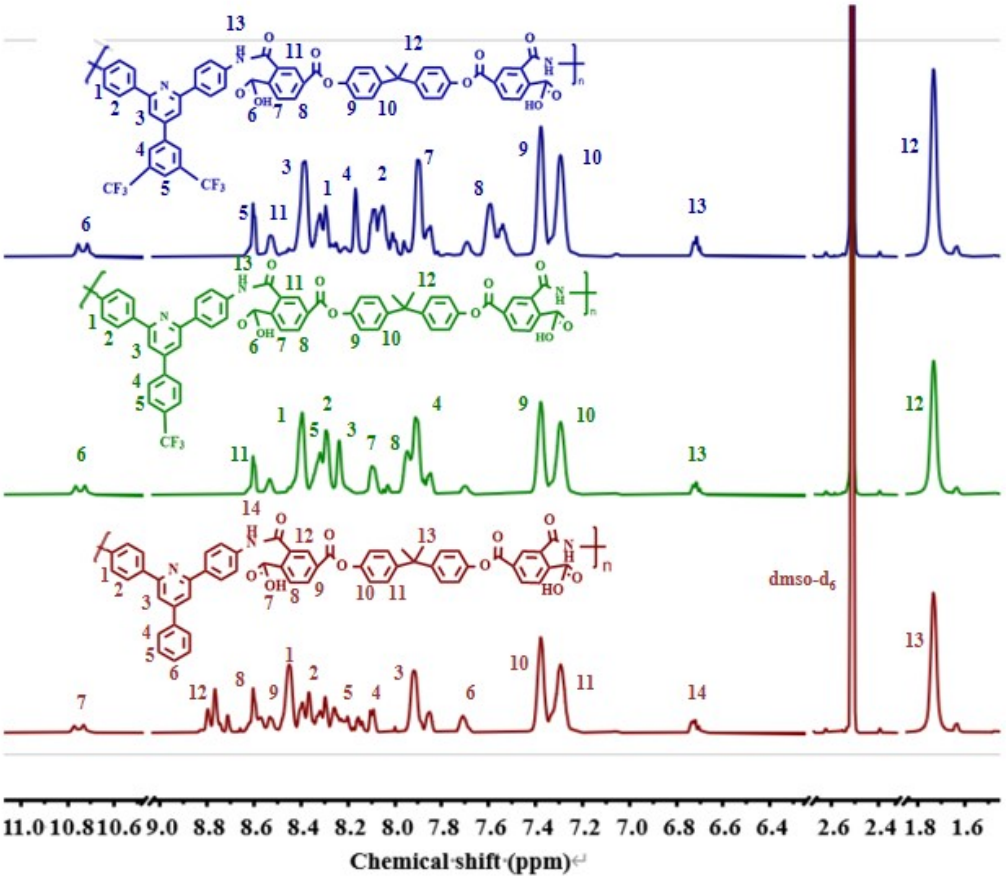

Figure S3. ^{1}H NMR spectra of PAAs in DMSO-d_6

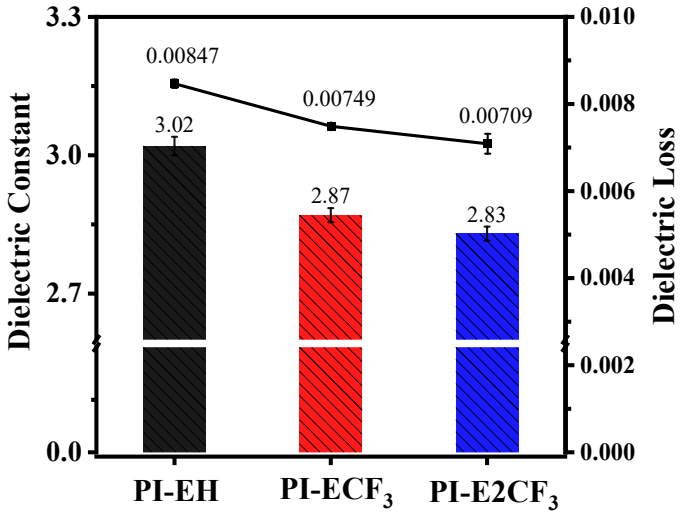

Figure S4. Dielectric properties of PI films under humid conditions

(a)

Results

Analysed by GPC at 21:15:30 on 2023年9月20日

Comments

Key Results

	Bulk MW (g/mol)	Mw (g/mol)	Mn (g/mol)	PD	Rgw (nm)	Rg Intercept	Rg Slope	Rhw (nm)
Peak 1	113363	98583	38893	2.535	0.00	NaN	NaN	10.11

Rh Intercept	Rh Slope
-1.381	0.4779

(b)

Results

Analysed by GPC at 21:00:32 on 2023年9月20日

Comments

Key Results

	Bulk MW (g/mol)	Mw (g/mol)	Mn (g/mol)	PD	Rgw (nm)	Rg Intercept	Rg Slope	Rhw (nm)
Peak 1	63358	63645	29182	2.181	0.00	NaN	NaN	8.49

Rh Intercept	Rh Slope
-1.342	0.4728

(c)

Results

Analysed by GPC at 21:13:21 on 2023年9月20日

Comments

Key Results

	Bulk MW (g/mol)	Mw (g/mol)	Mn (g/mol)	PD	Rgw (nm)	Rg Intercept	Rg Slope	Rhw (nm)
Peak 1	69233	69844	32352	2.159	0.01	16.2	-3.734	9.30

Rh Intercept	Rh Slope
-1.295	0.4673

Figure S5. (a) GPC Date of PI-EH-PAA; (b) GPC Date of PI-ECF_3-PAA;(c) GPC Date of PI-E2CF_3-PAA